Scholar Publishing Group
International Journal of Engineering Technology and Construction
https://doi.org/10.38007/IJETC.2022.030301
ISSN 2789-7176 Vol. 3, Issue 3: 1-19

Temperature Regulation Performance of Arc Sprayed Nano-Sealed Composite Coating in a Simulated Green Building Environment

Depak Kumar Jaine*

Chongqing University of Posts and Telecommunications, China

**corresponding author*

Keywords: Steel Bridge, Arc Spraying, Nano-Modified Coating, Concentrated Slurry, Seal Coating

Abstract: In recent years, due to the continuous development of industry, there is an increasing demand for special materials. Especially in the petroleum, chemical, machinery and other industries, higher requirements for materials with comprehensive new properties have been put forward. In addition to meeting the strength, toughness, shaping, and impact properties of the material, it must also meet the conditions of wear and corrosion resistance of steel materials in special environments. Among them, arc spraying technology is an important branch of thermal spraying technology in the emerging surface engineering discipline, and it has excellent temperature regulation performance when used in a simulated green building environment. The purpose of this paper is to study the temperature regulation performance of the arc sprayed nano-closed composite coating in a simulated green building environment. In this paper, arc spraying nano-material concentrates and nano-coatings are prepared, and nano-modified epoxy sealing coatings for sealing of metal coatings in arc-spraying are developed. In this paper, the thermoregulation performance of spray coatings is studied by simulating a green building environment. Experimental results show that the coating can still maintain the room temperature at about 16 degrees when the outdoor temperature exceeds 30 degrees celsius. It can be seen that the use of the spray-coated insulation board is beneficial to reduce the difference in indoor temperature at the same time, is beneficial to the uniform distribution of indoor temperature, and can effectively slow down the fluctuation of indoor temperature.

1. Introduction

As the society pays more and more attention to environmental protection, the lightweight of materials has become the focus of attention of all countries in the world. The arc spraying process is an important part of the engineering discipline, and it has been a very mature process. It has been

widely used in the industrial field in many countries and has attracted more and more people's attention. With the continuous development and improvement of arc spraying technology, it plays an important role in large-area spraying of long-term protective coatings. The arc sprayed nano-closed composite coating has good high temperature resistance, corrosion resistance, wear resistance, and high hardness. It can play a huge role in the field of green buildings through a certain preparation process [1].

The arc spray coating generally goes through a process of heating→ melting→ accelerating→ impacting the substrate→ cooling and solidifying→ forming the coating [2]. The development of arc spraying technology to this day has not only made long-term anti-corrosion in the fields of petroleum, machinery, and chemical engineering, but also made great progress in the repair of parts and the wear resistance of large transport aircraft. Adding certain ingredients to the spray material can increase the heat capacity of the building components, reduce the cold/heat load of the building, realize the transfer of peak load, and help maintain a comfortable indoor temperature environment. The arc spraying nano-sealed composite coating has a dense and firm structure, good strength and toughness, and good thermal properties. Especially under the natural convection conditions that change with temperature, the spraying material has a good prospect for architectural applications.

Regarding the research of arc spraying technology, many scholars at home and abroad have conducted multi-angle research on it. R, H, Singleton and others successfully prepared Fe-Al alloy coating on the surface of structural steel by plasma spraying technology, and the results showed that the hardness of Fe-Al alloy coating is 7.6GPa, which is relatively high [3]. Bobzin K uses high velocity arc spraying (HVAS) technology to obtain Fe-Al coatings with better performance by adding different elements to the powder core material [4]. Kuznetsov YA uses transmission electron microscope (TEM), scanning electron microscope (SEM) and THT07-135 high temperature wear equipment to analyze the microstructure and abrasive wear performance of the coating. It is found that adding Cr_3C_2 can greatly increase the room temperature wear behavior. Fe-Al/WC coating The layer has an adaptation period at the beginning of the abrasion experiment [5]. As the temperature increases, the wear resistance of the $Fe-Al/Cr_3C_2$ coating becomes unstable when it changes from room temperature to 250℃, and then becomes stable from 250℃ to 550℃; the wear resistance of Fe-Al/WC changes with the increase of temperature Very good. Bobzin K uses the characteristics of thermal spraying powder core wire to control the composition and adding certain B and Zr to FeAl wire to improve the plasticity of the coating [6]. This is due to the combination of B and Zr particles in the thermal coating process to produce ZrB_2 which can refine the grains of the coating and improve the performance of the coating. B has the function of strengthening the grain boundary, refining the grains, improving the strength and toughness of the material, and preventing the intergranular fracture of the alloy. Gusev VM uses the control of the amount of liquid fuel in the combustion chamber of the supersonic flame spray gun to change the flying speed of the droplet to prepare FeAl Coating [7]. The results show that the higher the flying speed of the sprayed particles, the finer the droplets, the more fully the powder material burns, the less undissolved particles contained in the coating, the better the compactness of the coating, and the more uniform structure. The content of oxides is also lower than the flying speed of sprayed particles.

The innovations of this paper are: preparing the arc spraying nano-material concentrate and nano-coating, and developing the nano-modified epoxy sealing coating for the sealing of the arc-spraying metal coating; aiming at the characteristics of green buildings, combining mechanical design theory and surface engineering technology, through multiple atomization jet technology

research, developed a mechanized high-efficiency multi-atomization arc spraying system to solve the problems of low spraying construction efficiency, narrow spray range, low coating adhesion, uneven thickness and unstable quality, and realize spraying the width is 140mm, the current is 700A, the construction efficiency is increased by 2 times, the coating adhesion is increased by 40%, the coating thickness is more uniform, and the quality is more stable.

2. Temperature Regulation Performance of Arc Sprayed Nano-Closed Composite Coating in a Simulated Green Building Environment

2.1 Spraying Equipment

The arc spraying equipment is shown in Figure 1, and consists of a rectifier power supply, wire feeding device, control device, spray gun and compressed air supply system. As shown in Figure 1, the supporting equipment includes SB10-H wire feeder and XTQ-1 spray gun. This equipment has two wire feeding methods, back push and front pull, and is a new generation product with high efficiency and low energy consumption. The compressed air supply system is a KAISERS200 piston air compressor.

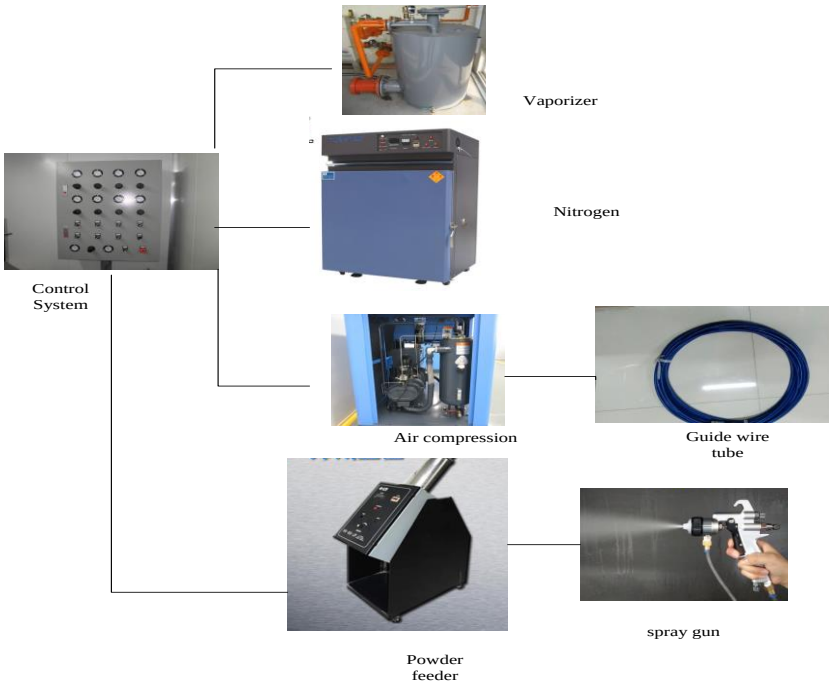

Figure 1 Arc spraying equipment

2.2 Design Of Atomizing Nozzle

The optimized design of the atomizing nozzle can achieve a higher impact velocity of atomized particles and a good atomization effect, and improve the performance of the arc sprayed layer. Among them, all sides of the wire ends of the spray gun are exposed to the compressed air jet, so that the droplets of the metal wire are atomized, the particle size is reduced, and the coating structure is refined [8].

The calculation of the characteristic parameters (throat diameter and outlet diameter) of Laval nozzles needs to pay attention to the following points:

(1) Because the nozzle is short and the airflow velocity is high, the boundary layer formed by the airflow inside the nozzle is very thin, and the viscosity has little effect on the flow, so the viscosity of the air flow is not considered, and the non-viscous flow is treated.

(2) The contact time between the atomizing airflow and the nozzle is very short, and the heat transfer between them can be ignored. Only the main factor of cross-section change is considered, and the law of flow changes with cross-section is calculated according to isentropic flow.

(3) Calculation of characteristic parameters:

The inlet parameters of the Laval nozzle are mainly the state parameters of the gas source, the inlet pressure, the inlet temperature, and the inlet flow rate of the gas flow. According to the relevant equations of aerodynamics and these parameters, the Laval nozzle can be designed [9]. The stagnation parameters of the airflow: stagnation temperature T_O, stagnation pressure P_O, as shown in formulas (1) and (2):

$$T_O = T_1 + \frac{1}{2C_{\mathrm{p}}} V_1^2 \tag{1}$$

$$P_O = P_1 \left[\frac{T_0}{T_1} \right]^{y/(y-1)} \tag{2}$$

In formulas (1) and (2), T_1, V_1 , P_1 are the temperature, velocity and pressure of the inlet airflow, C_{p} is the specific heat capacity at constant pressure, and y is a constant. From the following formulas, the critical velocity V_c, the exit velocity V_2, the exit Mach number M_{a}, the exit diameter D_2 and the critical diameter D_c can be obtained respectively.

When the flow velocity in the tube and nozzle reaches the speed of pressure wave propagation in this state, that is, the speed of sound, the flow velocity remains unchanged no matter how much the downstream pressure decreases. The speed at which the flow reaches this critical condition is called the critical velocity. The calculation method of critical speed V_c is shown in formula (3)

$$V_c = \sqrt{\frac{2yRT_O}{\mathrm{y}+1}} \tag{3}$$

The calculation method of critical cross-sectional area A_c is shown in formula (4):

$$A_c = \frac{M}{\sqrt{\frac{2y}{\mathrm{y}+1}\left(\frac{2}{\lambda+1}\right)^{\frac{2}{\mathrm{y}-1}} RT_0}} \tag{4}$$

The calculation method of critical diameter D_c is shown in formula (5):

$$D_c = \sqrt{\frac{4A_c}{\pi}} \tag{5}$$

At the outlet, the airflow velocity rises to the maximum and the airflow pressure drops to the

back pressure. The outlet velocity V_2, the outlet Mach number V_2, and the critical cross-sectional area A_2 are calculated as shown in formulas (6), (7), and (8):

$$V_2 = \sqrt{\frac{2}{\text{y-1}} RT_O \left[1-(\frac{P_e}{P_O})^{1-\frac{1}{y}}\right]} \quad (6)$$

$$M_a = \sqrt{\frac{2}{\text{y-1}} \left[(\frac{P_o}{P_2})^{1-\frac{1}{y}} - 1\right]} \quad (7)$$

(The nozzle outlet mach number M_a is determined by the ratio of the neck area to the outlet area and the ratio of the retention pressure to the outlet pressure.)

$$A_2 = \frac{M}{\sqrt{\frac{2y}{\text{y-1}} \left[(\frac{P_e}{P_O})^{\frac{2}{y}} - (\frac{P_e}{P_O})^{\frac{y+1}{y}}\right]}} \quad (8)$$

The outlet diameter calculation method is shown in formula (9):

$$D_2 = \sqrt{\frac{4A_2}{\pi}} \quad (9)$$

In formula (9), throat diameter and outlet diameter D_2 are the key parameters of Laval nozzle. During the flow of the atomized airflow from the inlet to the outlet of the laval nozzle, the pressure energy, kinetic energy, and internal energy change regularly along the nozzle, the pressure and temperature continue to decrease, and the speed continues to increase.

(4) Nozzle profile design

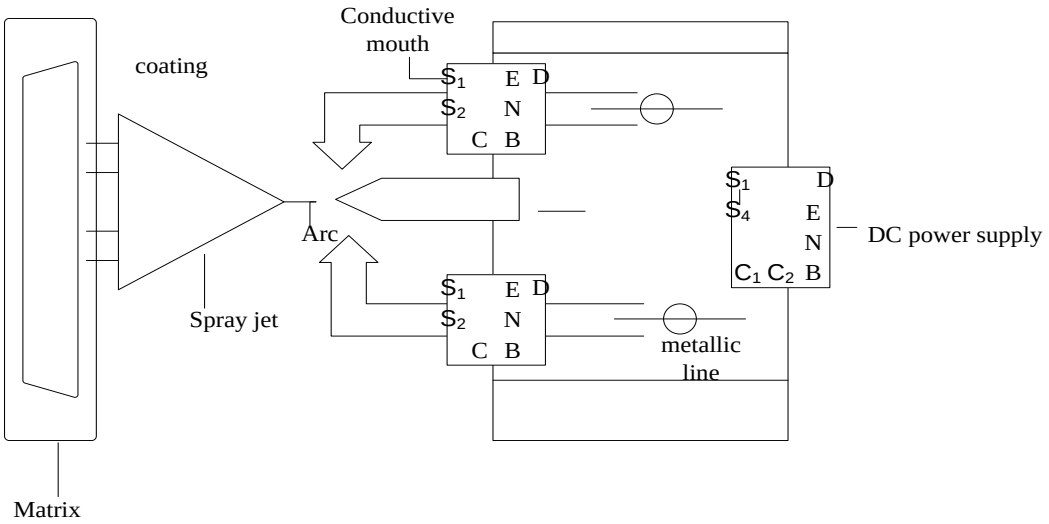

Figure 2 Schematic diagram of arc spraying principle

The principle of arc spraying is shown in Figure 2, where the design of the nozzle requires special attention. After the nozzle's characteristic parameters throat diameter and outlet diameter are calculated, the nozzle profile design can be carried out. The profile design mainly considers: the longer the nozzle, the longer the acceleration process of the airflow on the sprayed particles, which is conducive to the speed of the particles. Improved; when the nozzle profile design is not appropriate, shock waves may be formed in the nozzle, which will cause energy loss of airflow and sprayed particles, which will affect the atomization and acceleration; the transition of each section of the nozzle inner wall should be smooth to avoid shock wave, the surface roughness inside the nozzle should be low to reduce friction loss, and the nozzle outlet should be kept sharp to avoid gas wall separation [10].

2.3 Optimized Design of Arc Spray Gun Spraying Trajectory

The thickness and thickness uniformity of the arc sprayed coating is a key index to evaluate the quality of the coating. For the temperature-regulating spray coating of green buildings, the thickness of the spray coating is required to meet the design requirements and the thickness uniformity is good. If the coating thickness is too thin, it will not meet the expected temperature regulation requirements. If the coating is too thick, materials will be wasted. Excessive consumption of materials will increase production costs and reduce economic benefits.

Similarly, for the paint coating behind the metal spray coating, its thickness and uniformity also have a very large impact on the quality of the coating. The color saturation and vividness of the arc sprayed composite coating, especially the topcoat, are closely related to the thickness of the coating. The topcoat should have enough thickness to cover the unevenness of the primer or the surface of the workpiece [11]. A coating that is too thick will have a tendency to crack during use and will also cause excessive consumption of materials.

(1) Optimization design method of spray gun spraying trajectory-complex free-form surface spraying trajectory planning

In order to improve the spraying efficiency and ensure the uniformity of the paint film, automatic trajectory planning has become a hot research object. The computer can dynamically generate the spraying trajectory through reliable algorithms, simulate and analyze the processing process in the three-dimensional simulation interface, and finally generate the robot control program. This process is called computer offline programming [12]. Compared with online programming, offline programming has many advantages. First of all, the computer completes the trajectory planning of the next workpiece during the machining process without stopping the machining process. Secondly, the planned trajectory with simulation software can simulate the processing process in the computer to observe the processing accuracy, paint film thickness, and spray uniformity of the planned trajectory [13]. When the workpiece type needs to be changed, there is no need to teach again like online programming, only the corresponding program needs to be modified in the computer, which further improves the spraying efficiency.

It can be seen from the comparison that the use of offline programming can improve the effect of spraying. In production engineering, it is difficult to plan the spraying trajectory of complex free-form surfaces. When using the currently commonly used slicing method for trajectory planning, it will encounter the situation that the planning effect is not good when the curvature of the surface is large. This path method is adopted although the planning effect is better, the algorithm is too complicated.

Aiming at the problem of complex free-form surfaces that are difficult to accurately plan, the

STL slicing method is used for trajectory planning. The algorithm idea is as follows:

First, read and display the STL model of the sprayed workpiece in the 3D simulation interface, then determine the slicing direction according to the direction of motion of the spray gun, and use several parallel planes to slice the model;

Then, solve all the intersection points where the tangent plane intersects the model, and solve the normal vector of each intersection point, connect all the intersection points in order to obtain the profile information of the tangent plane section; offset by the external normal vector to get the spray gun motion trajectory;

Finally, combined with the relevant information of the robot, the trajectory is post-processed and converted into a motion control program that the robot can recognize. The algorithm steps are shown in Figure 3:

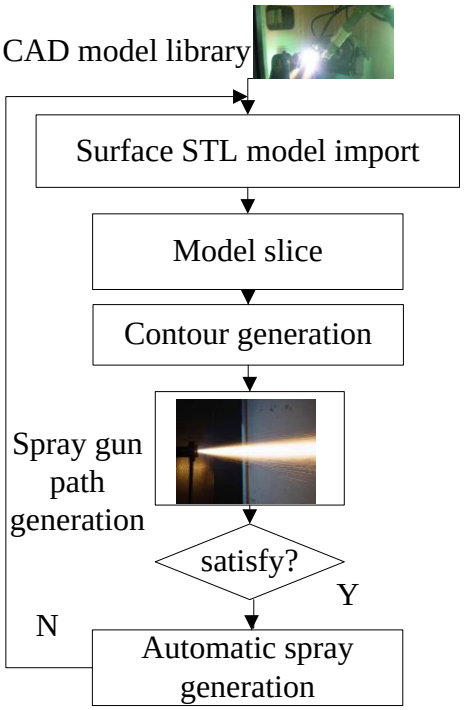

Figure 3 Slicing algorithm generation

The algorithm framework is shown in Figure 3. The main steps of the algorithm are summarized as follows:

First, calculate the total number of triangles. Observing from the definition of the character format, we can see that the number of ASCII lines occupied by each triangle is 7 lines. Therefore, after reading the number of lines, divide by 7 to get the number of triangles k.

Then, set the number of layers i=1. Next, search for facet, normal, ni, nj, nk, store the normal vector information, search for the outer loop, read and store the coordinates of the three vertices through the vertes loop. And search for the end facet, which proves that the currently read triangle face has been stored, i=i+1, and finally repeat the above two steps until i=k and the algorithm is completed.

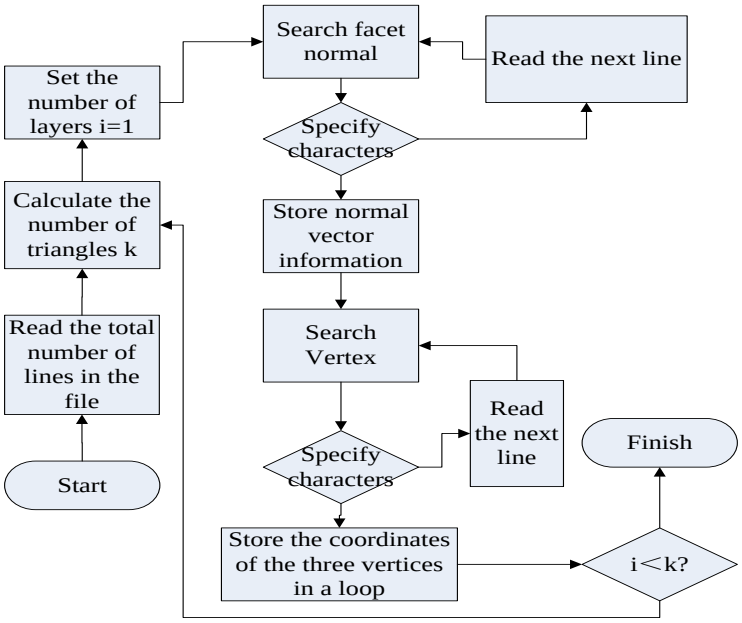

Figure 4 STL file reading algorithm flow chart

(2) Spray gun spraying trajectory optimization design method-spray gun trajectory optimization on the plane

In the actual painting operation, the spray gun moves on the workpiece at a uniform speed to form a uniform paint film on the surface of the workpiece [14]. Due to the large width of the workpiece, it is usually impossible to cover the workpiece in one spray, and the spray gun is required to spray back and forth according to the planned path. In the multi-pass spraying process, there are overlapping areas between adjacent spraying tracks. In order to obtain a uniform paint film thickness, the size of the overlapping area needs to be reasonably planned to avoid the difference between the paint film thickness in the overlapping area and the paint film thickness in the non-overlapping spray area If it is too large, it will affect the overall uniformity of the coating.

2.4 Nano Material Concentrate and Preparation Process

The concentrated slurry of nanomaterials can be divided into resin-free type and resin-containing type. The resin-free nano-material concentrate can be added to any resin coating system, but it is difficult to promote at present due to the difficulty in designing the formulation of the nano-concentrate and the short storage period. The formulation design of the resin-based nano-material concentrate is easy to realize, with good dispersion effect and stability, and long storage period. However, it is usually only suitable for the same type of resin coating system. Compatibility tests are required before adding different types of resin coating systems [15].

(1) The basic requirements of nano-material concentrates:

The nanomaterial concentrate should meet the following basic requirements:

1) The resin content should not be too high, generally not more than 30%;

2) Have the highest possible content of nanomaterials, generally not less than 15%;

2) The compatibility with the resin of the matching coating system is better;

3) The solvent content cannot be too high, and the viscosity of the slurry cannot be too low;

4) During the storage period, it will not sink to the bottom, do not seep liquid, and will not dry

up;

5) The dispersion stability of nanomaterials should be good, and there will be no delamination, no return to coarseness, and no flocculation during the storage period;

6) The production process is not complicated, it can be produced on a large scale, the quality is stable, and the reproducibility is good;

7) It has proper fluidity and can be pumped;

8) The use of concentrated slurry to produce coatings can significantly improve the overall performance of the coatings and has no adverse effects on durability;

9) The product is cost-effective, and the use of concentrated slurry to produce nanocomposite coatings will not greatly increase the cost.

To fully meet the above-mentioned basic requirements of concentrated slurry, appropriate additives and nanomaterials must be selected and used in the formulation design [16]. Without suitable additives, the content of nanomaterials in the concentrate will not be very large. Only by choosing appropriate nanomaterials and wetting and dispersing agents can the viscosity of the nanoconcentrate be reduced. By increasing the amount of nanomaterials added, it can maintain the dispersion stability and concentration of nanomaterials. The problem of thickening of the slurry occurs when the solvent is diluted when the paint is mixed and mixed [17].

(2) Typical components of nano-material concentrate

1) Nano materials

Nanomaterials are the most important component in the concentrate. The concentration of nanomaterials in the concentrate should be increased as much as possible, so that adding a small amount of nanomaterial concentrate can make the finished paint have a higher content of nanomaterials.

2) Additives

The second important component of nanomaterial concentrates is additives, including dispersants, anti-settling agents and defoamers. Among them, the dispersant is a component that must be added, and its main function is to reduce the viscosity of the nano-concentrate to obtain the highest possible nano-material content [18]. The choice of dispersant depends on its compatibility with the dispersion system and the required properties [19]. The function of the anti-settling agent is to keep the concentrated slurry from sinking after long-term storage. The defoamer can eliminate the air bubbles generated during the production of concentrates and coatings.

3) Grinding resin

The grinding resin can be the same resin as the coating system, or it can be a special grinding resin for masterbatch, which is mainly selected according to the compatibility with the coating system [20]. The amount of grinding resin in the concentrate should be as low as possible. When a good dispersant is used as a wetting and dispersing additive for nanomaterials to produce nano-concentrates, grinding resins can also be eliminated or used less.

4) Solvent

In addition to the solvent brought in by the grinding resin and dispersant, in the production of nano-concentrates, a solvent is also required as a dispersion medium to adjust the viscosity of the system [21]. The correct choice of solvent is important because it also affects the storage stability of nano-concentrates and involves whether it can meet the requirements of volatile organic compounds (VOC) regulations [22]. In general, a mixture of multiple inert solvents with suitable dissolving power should be selected.

2.5 Preparation Process of Arc Spraying Nano-Closed Composite Coating

(1) Surface treatment

The pretreatment condition of the base metal surface determines the bonding performance of the anti-corrosion coating and the base, and has an important influence on the service life of the anti-corrosion coating. The surface treatment process before the arc spraying anti-corrosion construction includes: removing dirt and grease on the steel surface; sandblasting and removing rust on the surface of the steel structure [23].

Sandblasting process parameters: air pressure 0.5~0.7MPa, spray angle 60~90, spray distance 200-300mm.

(2) Arc spraying

The high-efficiency multi-atomized arc spraying equipment is used to perform arc spraying on the workpieces after sandblasting and rust removal. The main process parameters are shown in Table 1.

Table 1 Process parameters of high-efficiency multi-atomization arc spraying equipment

Parameter category	Process parameters	
Spray material	Aluminum wire	Grade 1060 (GB/T3190-2008)
Power parameters	Spraying voltage	30~34V
	Spray current	300~600A
Atomization parameters	Atomizing gas pressure	0.5~0.7MPa
	Nozzle structure	Multiple atomizing nozzle
Operating parameters	Spraying distance	200±50mm
	Spray angle	60~90 °
	Spraying speed	2~3 times to reach the specified thickness
Base surface temperature	Workpiece temperature during spraying	≤100℃
Spraying environment	Workpiece surface temperature	≥ Dew point 3℃
	humidity	≤85%
	Air dust	without
	Wind force	Measures beyond 5 levels
Intermittent time	After sandblasting and rust removal to spraying time	≤4h
	Rainy days during the spraying process	≤2h
Coating quality	Appearance of sprayed aluminum layer	Uniform, dense, no leakage and weak adhesion
	Thickness of spray aluminum layer	Coating, no adhesion of large molten particles
	Cohesion of sprayed aluminum layer	200μm

3. Experimental Design of Temperature Regulation Performance of Arc Sprayed Nano-Closed Composite Coating in a Simulated Green Building Environment

3.1 Determination of the Bonding Strength of the High-Efficiency Multi-Atomized Arc Spray Coating

(1) Test purpose: by measuring the improvement of the bonding strength between the spray coating and the substrate, to indirectly judge the quality of the multi-atomizing jet velocity and the atomizing effect. If the spraying speed is fast, the bonding strength between the coating and the substrate will be high; if the atomization effect is good, the coating will be dense and the cohesive strength of the coating will be high.

(2) Test method: According to the test method specified in "GB/T8642-2002 Thermal Spraying Tensile Bonding Strength Determination" standard, conduct high-efficiency multi-atomized arc spraying zinc/aluminum coating and substrate bond strength test, and conduct ordinary arc at the same time, the bond strength test of spray gun spraying zinc/aluminum coating and steel substrate for comparison [24]. According to the requirements of national standards, the bonding force test sample adopts two standard dual samples A and B of $\phi 40\times 50$, in which the end face of A is sandblasted at level $Sa3$ and then arc sprayed, and the end face of sample B is sandblasted at level $Sa3$, which is generally cured at 25℃ 24h is fine. In order to ensure a satisfactory curing effect, the bonded sample can be kept at 60~80℃ for 1~3h. The fully cured sample was pulled apart with a hydraulic tensile testing machine, and the bonding strength between the coating and the substrate was measured.

(3) Test equipment: self-made high-efficiency multi-atomized arc spraying equipment, and commercially available ordinary arc spraying equipment.

(4) High-efficiency multi-atomized arc spraying equipment parameters: no-load voltage 34V, spraying current 500A, spraying distance 200mm, air pressure 0.55Mpa, spraying six sets of samples, including 3 sets of zinc spray and 3 sets of aluminum spray.

(5) Ordinary arc spraying equipment: no-load voltage 34V, spraying current 200A, spraying distance 200mm, air pressure 0.55Mpa, spraying four sets of samples, including two sets of zinc spray and two aluminum sprays.

3.2 Experimental Design of the Microstructure of the High-Efficiency Multi-Atomized Arc Spray Coating

Experimental purpose: to investigate the microstructure and surface morphology of the multi-atomized spray coating, and indirectly evaluate the atomization effect.

Experimental instrument: Scanning electron microscope (SEM), CambridgeStereoscan250Mk3 type.

Experimental method: The microstructure and surface morphology of the bonding interface between the multi-atomized arc sprayed aluminum coating and the steel substrate were analyzed by scanning electron microscopy. At the same time, the bonding surface structure of the ordinary single-atomized arc sprayed aluminum coating was analyzed.

3.3 Preparation Process of Nano-Material Concentrate

The material in this study is a solvent-based epoxy resin system nano-oxide material

concentrated slurry, which has the characteristics of high solid content, moderate viscosity, good dispersion, and good stability. The preparation process of the nano-sized slurry is as follows:

(1) Preparation of raw materials: Weigh each component according to the design of the formula, and ensure that the water content in the solvent is low. If the nano oxide powder is damp, it needs to be dried and dehydrated in advance.

(2) Feeding and pre-dispersion: first mix the mixed solvent and epoxy resin and stir evenly at low speed (200-600rpm), add dispersant and/or hyperdispersant until it is evenly stirred, add defoamer until it is evenly stirred, and then the measured inorganic nano-oxide material is slowly added at 400-800rpm speed, added in batches, and added while stirring. After all is added, continue to stir for 5-10min, and then add anti-settling agent and under low-speed stirring. The remaining amount of solvent (adjust the viscosity of the slurry to be moderate);

(3) High-speed dispersion: use a high-speed or high-shear disperser (above 5000r/min) for strong dispersion for 1 hour;

(4) Grinding and dispersion: sanding with a sand mill (speed above 2000rpm) for 15-3h (or grinding with a ball mill for 4h);

(5) After filtering, it is packed into barrels to make nano-material concentrated slurry.

3.4 Preparation Process of Nano-Material Concentrate

The dispersion process of inorganic nano-powder in the preparation of solvent-based epoxy resin system nano-concentrate is shown in Figure 5. A good dispersion of nano-powder in resin solution requires three basic processes, namely wetting process and separation process.

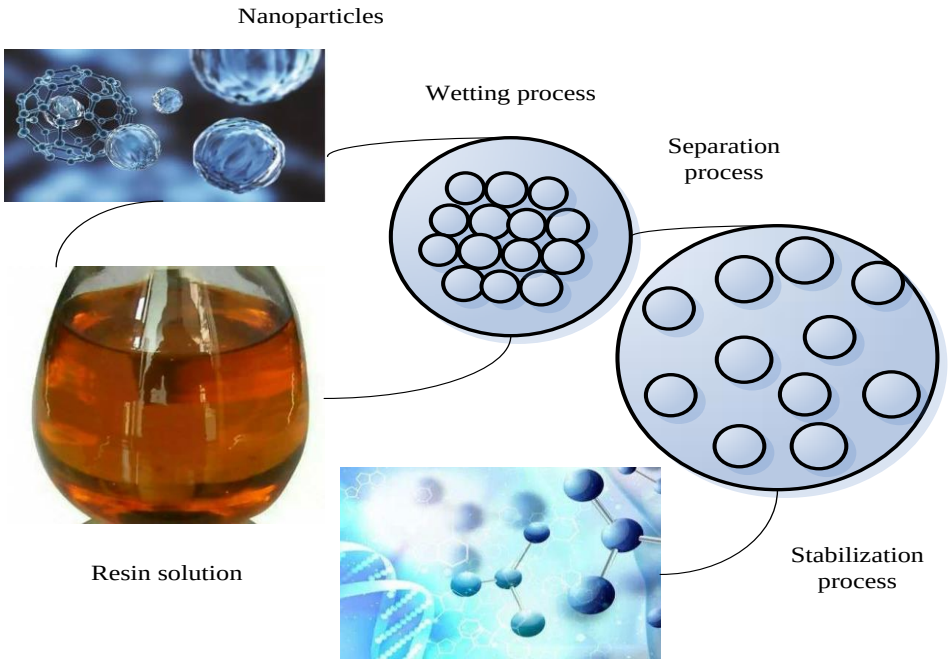

Figure 5 Wetting, separation and stabilization process of nanomaterials in resin solution

3.5 Experimental Design of Arc Spraying Nano-Closed Composite Coating

(1) Test purpose

By testing the bonding strength of the multi-atomized arc sprayed aluminum coating and the

substrate, the bonding strength of the nano epoxy sealer and the sprayed aluminum coating, and the interlayer bonding strength between the nano-closed bottom and the top coat, we can learn about the arc spraying nano-sealing The overall bond strength of the composite coating. Take common arc spray aluminum coating and traditional anti-corrosion coating samples as control.

(2) Test equipment

Self-made 1 high-efficiency multi-atomized arc spraying equipment, 1 commercially available ordinary arc spraying equipment, and 1 universal electronic tensile testing machine.

(3) Coating sample preparation

Sample size and quantity: 10 pairs of standard samples of φ40X50mm, 60 pieces of Q235 steel plate of 150mmX70mmX3mm (rounded corners).

Surface treatment: the effective surface of all samples is sandblasted to remove rust Sa3 grade, Rz25-100um.

Arc spraying aluminum: 5 φ40 cylindrical dual samples and 30 Q235 steel plates are sprayed with high-efficiency multi-atomization arc spray guns,

(4) Experimental method

1) Bond the aluminum-blasted cylindrical dual sample and the sandblasted cylindrical sample with high-strength epoxy glue and cure naturally for 24 hours.

2) Apply a coat of nano-modified epoxy sealer 912 on both sides of 25 aluminum sprayed test panels and 25 sandblasted test panels, with a dry film thickness of 20-40um.

3) Apply a coat of commercially available epoxy seal primer 269 on both sides of 5 aluminum sprayed test panels and 5 sandblasted test panels, with a dry film thickness of 2040um.

4) 15 (sprayed aluminum + nano sealing paint 912) test panels and 15 (sandblasting + nano sealing paint 912) test panels, after the nano sealing paint 912 is dried for 24 hours, then apply 2 nano-modifications on both sides Epoxy intermediate paint 812, the dry film thickness of the intermediate paint is 80-100um.

5) 5 (spray aluminum + epoxy primer 269) test panels and 5 (sandblast + epoxy primer 269) test panels, after epoxy primer 269 is dried for 24 hours, and then painted on both sides for 2 coats epoxy mica intermediate paint 842, the dry film thickness of the intermediate paint is 80-100um.

6) 5 (spray aluminum + nano seal paint 912 + nano intermediate paint 812) test panels and 5 (sandblast + nano seal paint 912 + nano intermediate paint 812) test panels, after the nano intermediate paint 812 is dried for 24 hours, Then apply 2 coats of nano-modified fluorine-containing polyurethane topcoat 712 on both sides, and the dry film thickness of the topcoat is 80um.

7) Put 5 (sprayed aluminum + epoxy primer 269 + epoxy intermediate paint 842) test panels and 5 (sandblast + epoxy primer 269 + epoxy intermediate paint 842) test panels in the epoxy after the intermediate paint 842 is dried for 24 hours, two coats of acrylic polyurethane topcoat 990 are applied on both sides, and the dry film thickness of the topcoat is 80um.

3.6 Experimental Device for Simulating Green Building

The internal space of the simulated building is 0.5m×0.3m×0.3m. The side walls are made of 1cm plexiglass panels and 4cm polystyrene insulation layer, and the bottom is a 10cm thick polystyrene insulation layer. The top is a temperature control module of 0.5m×0.3m×0.02m, and polystyrene insulation is used around the module to simulate an actual building with a temperature control module; in addition, the outside of the insulation layer on the wall of the device is wrapped with tin foil to reduce solar radiation to the experiment the impact of the device.

During the experiment, a graphene heater with a rated voltage of 5V and a rated power of 1.5W was used to simulate the hourly cooling load caused by the heat dissipation of the indoor human body, lighting and equipment; in addition, because the temperature control module cannot meet the indoor heating demand at night in winter, additional the heating device simulates the heating equipment in the building.

During the experiment, the device was placed on the roof without any obstruction, and the temperature inspection instrument with its own storage function was used to record the temperature of each measuring point, and a small weather station was used to record the meteorological data, including dry bulb temperature, dew point temperature, humidity, wind speed and solar radiation, the recording time interval is 5 minutes.

4. Analysis of Temperature Regulation Performance of Arc Sprayed Nano-Closed Composite Coating in a Simulated Green Building Environment

4.1 Hardness of the Arc Sprayed Nano-Closed Composite Coating

The microhardness distribution of the coating is uneven, and the hardness values of different areas are different. In the experiment, select 5 areas for each coating sample to get the average value. The microhardness values of the four iron-based coating samples and the 45 steels plate are shown in Figure 6.

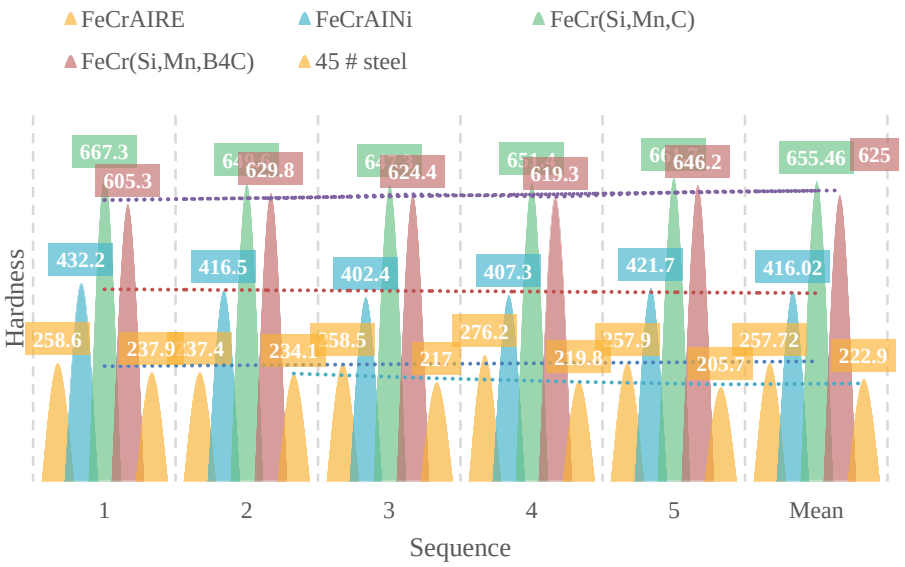

Figure 6 Hardness of arc sprayed nano-closed composite coating

Observing Figure 6, it can be found that the average hardness of the four iron-based coatings is higher than that of the 45 steel sample. Among them, the FeCr (Si, Mn, C) coating and FeCr (Si, Mn, B4C) prepared with two powder core wires. The hardness of the coating reaches more than 600HV, which is about 3 times that of the substrate sample, mainly because of the enhancement of the ceramic phase in the coating. The microhardness of the FeCrAIRE coating is slightly higher than that of the base sample, and the microhardness of the base coating FeCrAINi is about 1.9 times that of the base 45 steel sample. The FeCr (Si, Mn, B4C) coating and FeCr (Si, Mn, C) coating

prepared by powder core wire have the highest average hardness, both reaching more than 600HV.

4.2 Modeling Test of High-Efficiency Multi-Atomizing Nozzle

The high-efficiency multi-atomizing arc spray gun uses different atomizing nozzles to obtain different coating thickness distributions and the experimental data of the coating thickness distribution obtained by ordinary arc spray guns (the thickness measurement point interval is 10mm) is shown in Table 2.

Table 2 Coating thickness distribution

Serial number	Nozzle combination		Spraying process parameters	Coating appearance	Total width	Thickness distribution
1	1-A	2-A	32V/600A/200mm	Uniform and dense	160mm	45,85,130,160,135,125,140,113,116,117,150,158,153,135,121,75,40,44,46,42
2	1-A	2-B	32V/600A/200mm	Uniform and dense	160mm	60,93,124,120,143,127,124,115,115,120,115,126,115,110,115,90,54,53,57,59
3	1-B	2-A	32V/600A/200mm	Uniform and dense	160mm	60,100,140,163,154,145,129,146,130,136,131,178,175,175,120,100,62,57,59,56
4	1-B	2-B	32V/600A/200mm	Uniform and dense	160mm	61,105,124,125,132,124,127,118,123,116,142,125,123,124,117,109,67,63,59,57
5	Ordinary gun nozzle		32V/200A/200mm	Slightly dense	60mm	82,113,121,193,265,221,122,63,
6	Ordinary gun nozzle		32V/160A/200mm	Slightly dense	60mm	56,106,189,60,220,222,111,67
7	Ordinary gun nozzle		32V/150A/200mm	Slightly dense	60mm	50,93,142,223,265,214,83

The data of the thickness distribution of the multi-atomized arc spraying layer in Table 3 is made into a coating thickness distribution map, as shown in Figure 7.

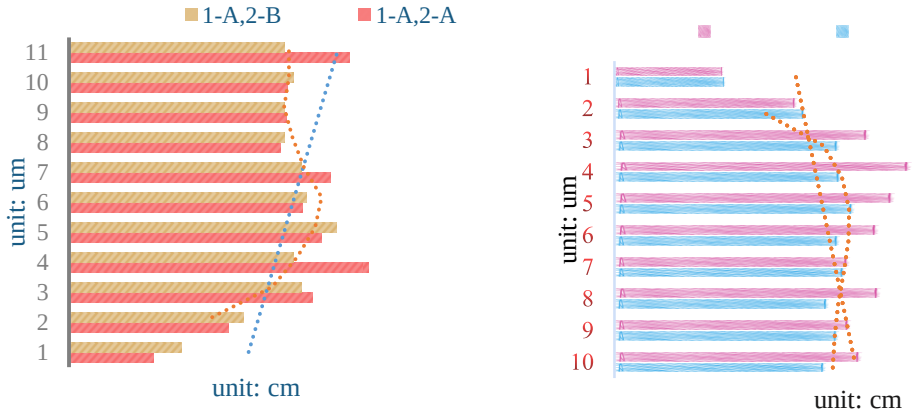

Figure 7 Thickness of multi-atomized arc spray coating

It can be seen from Figure 7 that the four nozzle combinations of the high-efficiency multi-atomization arc spraying equipment have achieved the goal of a total spraying width of 160mm and an effective spraying width of more than 120mm. At the same time, it can also be seen that the coating thickness distribution curve obtained by the nozzle combination of the first and third groups forms a curve of double hump; while the coating thickness distribution curve obtained by the nozzle combination of the second and fourth groups is more Better, the thickness fluctuation range is relatively small, and the effective coating width obtained by the fourth set of nozzle combination is the largest, reaching 140mm. Therefore, through experiments and analysis, the fourth nozzle combination (1-B+2-B) can be preliminarily selected as the stereotyped nozzle of the high-efficiency multi-atomization arc spraying equipment.

4.3 Determination of Air Consumption, Spraying Speed and Coating Deposition Rate

The test data records of air consumption, spraying speed and coating deposition rate are shown in Table 3.

Table 3. Air consumption, spraying speed and coating deposition rate data

name	1	2	3	4	5	6
	Spraying parameters U, I, L, P	Gas flow meter reading m^3/h	Weight of test piece before/after spraying Kg	Wire weight before/after spraying Kg	Zinc spray rate Kg/h	Coating deposition rate%
Ordinary spray gun	32V, 200A, 200mm, 0.55Mpa, spraying for 2min	80	8.540/8.960	6.240/6.990	22.5	56.0
Ordinary spray gun	32V, 600A, 200mm, 0.55Mpa, spraying for 2min	130	7.150/8.680	7.365/9.985	78.6	58.4

It can be found from Table 3 that the high-efficiency multi-atomization arc spray gun has two relatively independent air intake pipes, so it is understandable that the measured compressed air consumption is 62.5% higher than that of the ordinary spray gun. Compared with the 200A spraying current of the ordinary arc spray gun, the long-term normal spraying current of the high-efficiency multi-atomizing arc spray gun can reach 600A, and its zinc spraying speed also reaches 78.6kg/h, which is 349% of the spraying speed of the ordinary spray gun. The main reason for the increase in spraying speed is the increase in spraying current and wire feeding speed. The deposition efficiency of the high-efficiency multi-atomization arc spray gun is slightly higher than that of the ordinary arc spray gun. This is because although the atomization effect is improved, the arc spraying process determines that the coating deposition rate cannot be increased too much.

4.4 Temperature Control Characteristics

The air conditioner was used to adjust the temperature of the external environment during this experiment, and the temperature was set to 16℃. Figure 8 is the temperature change curve of the temperature measurement points on the lower surface of the insulation board. In the process of using infrared illuminators to heat the insulation board, the temperature rise rate of the insulation board first increases and then gradually decreases.

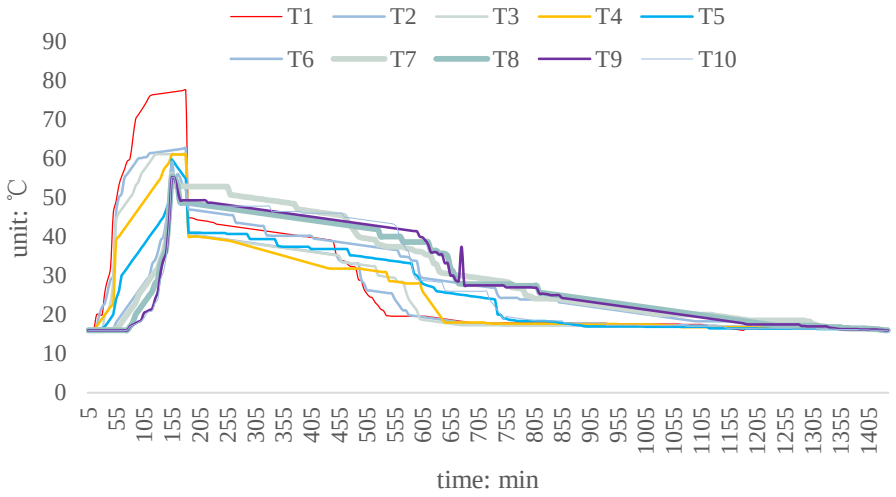

Figure 8 Temperature change curve of insulation board

Figure 8 shows the indoor temperature fluctuation curve of EP2 and EP2/CA (50%)-EP2/EHS (70%) experimental room. It can be seen from the figure that the use of the sprayed coating insulation board is beneficial to reduce the indoor temperature at the same time, the difference is conducive to the uniform distribution of indoor temperature and can effectively slow down the fluctuation of indoor temperature.

5. Conclusions

Aiming at the practical construction technology problems of traditional manual spraying equipment with low work efficiency, narrow spray range, low coating adhesion, uneven thickness and unstable quality, this paper combines mechanical design theory and surface engineering technology to develop a mechanized high-efficiency multi-atomizing arc spraying system, and through the two-step process of preparing nano-material concentrates and then nano-modified coatings, developed nano-modified epoxy sealing coatings for arc spraying metal coatings to seal holes. By simulating a green building environment, the temperature regulation performance of the spray coating is studied. The use of the coating energy is beneficial to reduce the difference in indoor temperature at the same time, and is beneficial to uniform distribution of indoor temperature.

References

[1] Smovzh D V , Sakhapov S Z , Zaikovskii A V , et al. Formation mechanism of MgO hollow nanospheres via calcination of C-MgO composite produced by electric arc spraying. Ceramics International, 2019, 45(6):7338-7343.

[2] Tamaki R , Yamakawa M . Effect of plate mounted between two wires in electric arc spraying.

Journal of computational science, 2019, 32(MAR.):56-67. https://doi.org/10.1016/j.jocs.2019.02.006

[3] R, H, Singleton, et al. Tungsten Fabrication by Arc Spraying. JOM, 2017, 13(7):483-486. https://doi.org/10.1007/BF03378087

[4] Bobzin K ,et al. Modeling Plasma–Particle Interaction in Multi-Arc Plasma Spraying. Journal of Thermal Spray Technology, 2017, 26(3):1-13. https://doi.org/10.1007/s11666-016-0514-5

[5] Kuznetsov Y A , Markov M A , Krasikov A V , et al. Formation of Wear- and Corrosion-Resistant Ceramic Coatings by Combined Technologies of Spraying and Micro-Arc Oxidation. Russian Journal of Applied Chemistry, 2019, 92(7):875-882.

[6] Bobzin K , Te M , Schein J , et al. Numerical Study on Plasma Jet and Particle Behavior in Multi-arc Plasma Spraying. Journal of Thermal Spray Technology, 2017, 26(5):811-830. https://doi.org/10.1007/s11666-017-0564-3

[7] Gusev V M , Elagina O Y , Nesterenko N S , et al. The Effect of the Design of the Nozzle System of Electric Arc Metallizing Devices on the Conditions of Spraying Wire Materials. Journal of Machinery Manufacture and Reliability, 2021, 50(3):185-190. https://doi.org/10.3103/S1052618821030055

[8] Arif Z , Shah M , EU Rehman, et al. Effect of spraying parameters on surface roughness, deposition efficiency, and microstructure of electric arc sprayed brass coating. International Journal of ADVANCED AND APPLIED SCIENCES, 2020, 7(7):25-39. https://doi.org/10.21833/ijaas.2020.07.004

[9] Nigam S , Mahapatra S S , Patel S K . Study of Various Aspects of Copper Coating on ABS Plastic by Electric Arc Spraying. Materials today: proceedings, 2018, 5(2):8446-8453. https://doi.org/10.1016/j.matpr.2017.11.540

[10] V. O. Royanov, Zakharova I . Applications of electric arc metallization method with pulsating air-spraying flow for application of coatings made from a cored wire. Reporter of the Priazovskyi State Technical University Section Technical sciences, 2020(40):44-50.

[11] Phanden R K , Sindhwani R , Kalsariya V , et al. Selection of material for electric arc spraying by using hierarchical entropy-TOPSIS approach. International Journal of Productivity and Quality Management, 2019, 26(3):276. https://doi.org/10.1504/IJPQM.2019.098364

[12] Santos L , Flores-Sahagun T S , Paredes R , et al. Study on the deposition of stainless steel on polymeric substrates by arc electric thermal spraying. Materials Research Express, 2019, 6(10):105314-. https://doi.org/10.1088/2053-1591/ab2a2f

[13] Zeng, Yong, Chen, et al. Spraying Trajectory Planning For Outer-Horn Surface With Two Patches Based On Continuous Varied Dip-Angle. International Journal of Robotics & Automation, 2018, 33(4):346-354.

[14] Pang X , Wang R , Wei Q , et al. Effect of epoxy resin sealing on corrosion resistance of arc spraying aluminium coating using cathode electrophoresis method. Materials Research Express, 2017, 5(1):016527. https://doi.org/10.1088/2053-1591/aaa055

[15] Zhe W , Du L , Hao L , et al. Preparation and characterization of YSZ abradable sealing coating through mixed solution precursor plasma spraying. Ceramics International, 2019, 45(9):11802-11811.

[16] Wang Z , Du L Z , H Lan, et al. A novel technology of Sol precursor plasma spraying to obtain the ceramic matrix abradable sealing coating. Materials Letters, 2019, 253(Oct.15):226-229. https://doi.org/10.1016/j.matlet.2019.05.079

[17] Ardalan R B , Jamshidi N , Arabameri H , et al. Enhancing the permeability and abrasion resistance of concrete using colloidal nano-SiO 2 oxide and spraying nanosilicon practices.

Construction & Building Materials, 2017, 146(Aug.15):128-135.

[18] Dobrozhan O , Vorobiov S , Kurbatov D , et al. Structural properties and chemical composition of ZnO films deposited onto flexible substrates by spraying polyol mediated nanoinks. Superlattices and microstructures, 2020, 140(Apr.):106455.1-106455.10. https://doi.org/10.1016/j.spmi.2020.106455

[19] Guo K , Hu A , Wang K , et al. Effects of spraying nano-materials on the absorption of metal(loid)s in cucumber. Nanobiotechnology, IET, 2019, 13(7):712-719. https://doi.org/10.1049/iet-nbt.2019.0060

[20] Noaema A H , Leiby H R , Alhasany A R . Effect of Spraying Nano Fertilizers of Potassium and Boron on Growth and Yield of Wheat (Triticum aestivum L.). IOP Conference Series: Materials Science and, Engineering, 2020, 871(1):012012 (9pp).

[21] Wain-Martin A , Moran-Ruiz A , Laguna-Bercero M A , et al. SOFC cathodic layers using wet powder spraying technique with self synthesized nanopowders. International journal of hydrogen energy, 2019, 44(14):7555-7563. https://doi.org/10.1016/j.ijhydene.2019.01.220

[22] An Y , Li S , Hou G , et al. Mechanical and tribological properties of nano/micro composite alumina coatings fabricated by atmospheric plasma spraying. Ceramics International, 2017, 43(6):5319-5328. https://doi.org/10.1016/j.ceramint.2017.01.072

[23] Chen X , Zhang B , Gong Y , et al. Mechanical properties of nanodiamond-reinforced hydroxyapatite composite coatings deposited by suspension plasma spraying. Applied Surface Science, 2018, 439(MAY1):60-65. https://doi.org/10.1016/j.apsusc.2018.01.014

[24] Potekaev A I , Lysak I A , Malinovskaya T D , et al. Coatings Based on Nanodispersed Oxide Materials Produced by the Method of Pneumatic Spraying. Russian Physics Journal, 2018, 60(11):2047-2049. https://doi.org/10.1007/s11182-018-1324-7